*Acta Cryst.* (1984). B40, 180–185

# A Molybdosilicophosphate with an Intersecting-Tunnel Structure which Exhibits Ion-Exchange Properties, $AMo_3P_{5\cdot8}Si_2O_{25}$ ($A$ = Rb, Tl)

By A. Leclaire, J. C. Monier and B. Raveau

*Laboratoire de Cristallographie, Chimie et Physique des Solides associé au CNRS, LA* 251, *ISMRA, Université de Caen, Esplanade de la Paix,* 14032 *Caen CEDEX, France*

(*Received* 24 *May* 1983; *accepted* 1 *November* 1983)


## Abstract

During an investigation of the system $A$–P–Si–Mo–O, the oxides $AMo_3P_{5\cdot8}Si_2O_{25}$ ($A$ = Rb, Tl) were isolated. They crystallize in space group $P\bar{3}1c$ with $Z = 2$. [Crystal data for $A$ = Rb: $M_r = 1009\cdot07$, $a = b = 8\cdot2905\,(10)$, $c = 17\cdot4390\,(23)$ Å, $V = 1038\cdot04$ Å$^3$, $D_x = 3\cdot266$ Mg m$^{-3}$, $\mu(\text{Mo } K\bar{\alpha}) = 4\cdot948$ mm$^{-1}$, $F(000) = 478$; for $A$ = Tl: $M_r = 1127\cdot97$, $a = b = 8\cdot2832\,(5)$, $c = 17\cdot4343\,(10)$ Å, $V = 1035\cdot92$ Å$^3$, $D_x = 3\cdot636$ Mg m$^{-3}$, $\mu(\text{Mo } K\bar{\alpha}) = 10\cdot248$ mm$^{-1}$, $F(000) = 522$; Mo $K\bar{\alpha}$ ($\lambda = 0\cdot71069$ Å), $T = 293$ K.] The structures were refined by full-matrix least-squares calculations to a final $R = 0\cdot031$ for Rb and $0\cdot054$ for Tl with 1191 (Rb) and 885 (Tl) measured independent reflections which had $I > 3\sigma(I)$. The three-dimensional framework of these oxides is built up from corner-sharing $MoO_6$ octahedra, $PO_4$ tetrahedra and $Si_2O_7$ groups forming an intersecting-tunnel structure. The ion-exchange properties of these oxides have been shown for the first time. Thus new oxides containing smaller ions such as $Na^+$ can be prepared without changing the lattice parameters.


## Introduction

Recent investigations of the P–W–O and $A$–P–W–O systems with $A$ = Na, K, Rb (Giroult, Goreaud, Labbé & Raveau, 1980, 1981*a*, *b*, 1982*a*, *b*; Hervieu & Raveau, 1982, 1983*a*, *b*; Domenges, Goreaud, Labbé & Raveau, 1982; Benmoussa, Labbé, Groult & Raveau, 1982) have shown that the ability of $PO_4$ tetrahedra and $WO_6$ octahedra to adapt to each other allows the formation of mixed frameworks built up from corner-sharing octahedra and tetrahedra. These oxides are original in that they exhibit, like $A_xWO_3$ tungsten bronzes, a tunnel structure (Magnéli, 1949, 1953; Magnéli & Blomberg, 1951; Banks & Goldstein, 1968; Swanson & Anderson, 1968; Kihlborg & Klug, 1973; Wanlass & Sienko, 1975; Hussain & Kihlborg, 1976; Kihlborg, Sundberg & Hussain, 1980; Kihlborg & Sharma, 1982). In this respect, Mo exhibits some similarity with W as shown by the $Mo^{VI}$ phosphates $(MoO_2)_2P_2O_7$, $MoO_2(PO_3)_2$ and $NaMoO_2PO_4$ (Kierkegaard, 1962*a*, *b*, *c*) and by the $Mo^{V}$ phosphates $(MoO)PO_4$ (Kierkegaard & Longo, 1970) and $(MoO)_2P_4O_{13}$ (Minacheva, Antsyshkina, Lavrov, Sakharova, Nikolaev & Porai-Koshits, 1979) whose structures are also formed of corner-sharing octahedra and tetrahedra; however, these oxides are not characterized by a tunnel structure. Nevertheless, a potassium molybdenum phosphate, $K_4Mo_8^{V}P_{12}O_{52}$, with a tunnel structure has recently been isolated (Leclaire, Monier & Raveau, 1983). No $Mo^{IV}$ phosphate has been obtained up to the present. Moreover, no molybdenum silicate or molybdosilicophosphate with a three-dimensional framework has been synthesized in spite of the ability of Si and Mo to form heteropolyanions as shown recently for $(CH_6N_3)_4SiMo_{12}O_{40}.H_2O$ (Ichida, Kobayashi & Sasaki, 1980) and $(NH_4)_{12}Cu_2Si_2Mo_{18}O_{66}.14H_2O$ (Fukushima, Kobayashi & Sasaki, 1981). For this reason, it was attractive to investigate the systems $A$–P–Si–Mo–O ($A$ = Rb, Tl). Thus, the present work deals with the crystallographic study of the oxide $AMo_3P_{5\cdot8}Si_2O_{25}$ ($A$ = Rb, Tl) which exhibits an intersecting-tunnel structure. The ion-exchange properties of these oxides have been shown for the first time.

## Determination of the structure

Mixtures of appropriate amounts of diammonium hydrogenphosphate $(NH_4)_2HPO_4$, carbonates $Rb_2CO_3$ or $Tl_2CO_3$ and oxides $MoO_3$, $SiO_2$ were first heated progressively up to 873 K in air in order to decompose the carbonates and the diammonium hydrogenphosphate. The resulting mixtures were then mixed with an appropriate amount of molybdenum, and heated at 1173 K in evacuated silica ampoules for several days. The composition of the black hexagonal crystals was determined by atomic absorption spectrometry and confirmed by electron microprobe analysis. A (00.1) hexagonal plate $0\cdot180 \times 0\cdot132 \times 0\cdot048$ mm for the Rb compound and a $(1\bar{1}.0)$ rectangular plate $0\cdot120 \times 0\cdot096 \times 0\cdot048$ mm for the Tl compound were selected for the structural determination.

The Laue patterns showed trigonal symmetry ($\bar{3}m$). The cell parameters in the *Abstract* were determined

0108-7681/84/030180-06$01.50 

by diffractometric techniques, with a least-squares refinement based on 25 reflections of reciprocal space.

The systematic absences in $hh\overline{2h}l$ for $l = 2n+1$ led to the space group $P31c$ or $P\bar{3}1c$. Both structures were solved and refined in the centrosymmetric $P\bar{3}1c$.

For both crystals, the data were collected on an Enraf–Nonius CAD-4 diffractometer with Mo $K\bar{\alpha}$ radiation filtered with a graphite monochromator. The intensities were measured up to $\theta = 45°$ with an $\omega$–$\frac{4}{3}\theta$ scan of $(0{\cdot}90 + 0{\cdot}35\,\mathrm{tg}\theta)°$ and a counter slit aperture of $(1{\cdot}0 + \mathrm{tg}\theta)$mm, all determined after a study of some reflections in the $\omega\theta$ plane.

The background intensity was measured on both sides of each reflection. A periodic intensity control verified the stability of the sample. 1191 and 885 independent reflections for the Rb and the Tl compounds respectively with $\sigma(I)/I < 0{\cdot}333$ were corrected for Lorentz and polarization effects; absorption corrections were applied using the program *AGNOSTC* (Coppens, Leiserowitz & Rabinovich, 1965; de Meulenaer & Tompa, 1965). Atomic coordinates of the $MoO_6$ groups were deduced from a three-dimensional Patterson map. The remaining atoms were located in subsequent Fourier synthesis.

The atomic parameters and an isotropic extinction parameter (Coppens & Hamilton, 1970) were refined by full-matrix least squares, and a linear weighting scheme $w = f(\sin\theta/\lambda)$ was adjusted by using the program *POND* (Leclaire, unpublished).

Scattering factors and anomalous-dispersion corrections for the different atoms of the compounds were taken from *International Tables for X-ray Crystallography* (1974).

The reliability factors were lowered to $R = 0{\cdot}031$ and $R_w = 0{\cdot}035$ with the extinction coefficient $g = 19\,(2)$ for the Rb compound and $R = 0{\cdot}054$ and $R_w = 0{\cdot}068$ with $g = 39\,(4)$ for the Tl compound. Final atomic parameters are given in Table 1.* The two sets of parameters are identical within the limits of the standard deviations.

## Description of the structure and discussion

Examination of the structure shows slices, perpendicular to the $c$ axis, containing all the tetrahedra and $\frac{2}{3}$ of the octahedra (Fig. 1*a*) lying between almost empty slices containing only the other octahedra and the Rb or Tl atoms (Fig. 1*b*). The host lattice of these oxides, which corresponds to the composition '$Mo_3P_6Si_2O_{25}$', is built up from corner-sharing $MoO_6$ octahedra, and $PO_4$ and $SiO_4$ tetrahedra, which delimit wide tunnels running along [100], [110] and

* Lists of structure factors and anisotropic thermal parameters have been deposited with the British Library Lending Division as Supplementary Publication No. SUP38960 (15 pp.). Copies may be obtained through The Executive Secretary, International Union of Crystallography, 5 Abbey Square, Chester CH1 2HU, England.

Table 1. *Atomic parameters for* $RbMo_3P_{5\cdot8}Si_2O_{25}$ *and* $TlMo_3P_{5\cdot8}Si_2O_{25}$

$$B_{eq} = \tfrac{4}{3}\textstyle\sum_i\sum_j \beta^{ij}\mathbf{a}_i\,.\,\mathbf{a}_j.$$

| | $x$ | $y$ | $z$ | $B_{eq}$(Å$^2$) |
|---|---|---|---|---|
| $RbMo_3P_{5\cdot8}Si_2O_{25}$ | | | | |
| Mo(1) | $\frac{1}{3}$ | $-\frac{1}{3}$ | 0·02239 (3) | 0·49 (0·01) |
| Mo(2) | $-\frac{1}{3}$ | $\frac{1}{3}$ | $\frac{1}{4}$ | 0·45 (0·01) |
| Rb | $\frac{1}{3}$ | $-\frac{1}{3}$ | $\frac{1}{4}$ | 4·46 (0·06) |
| P | 0·37854 (12) | 0·32971 (16) | 0·11067 (5) | 0·48 (0·02) |
| Si | 0 | 0 | 0·09078 (10) | 0·76 (0·03) |
| O(1) | 0·11371 (44) | −0·40782 (46) | 0·09504 (20) | 1·20 (0·08) |
| O(2) | −0·18867 (47) | 0·24728 (46) | 0·45370 (18) | 1·21 (0·08) |
| O(3) | 0·46708 (52) | 0·33313 (75) | 0·18697 (16) | 1·70 (0·10) |
| O(4) | 0 | 0 | 0 | 1·60 (0·15) |
| O(5) | 0·03300 (41) | −0·16308 (39) | 0·12389 (20) | 1·14 (0·07) |
| $TlMo_3P_{5\cdot8}Si_2O_{25}$ | | | | |
| Mo(1) | $\frac{1}{3}$ | $-\frac{1}{3}$ | 0·02220 (7) | 0·55 (0·02) |
| Mo(2) | $-\frac{1}{3}$ | $\frac{1}{3}$ | $\frac{1}{4}$ | 0·53 (0·03) |
| Tl | $\frac{1}{3}$ | $-\frac{1}{3}$ | $\frac{1}{4}$ | 5·77 (0·09) |
| P | 0·37818 (34) | 0·32978 (46) | 0·11045 (10) | 0·52 (0·05) |
| Si | 0 | 0 | 0·09101 (26) | 0·72 (0·07) |
| O(1) | 0·11354 (119) | −0·40731 (124) | 0·09473 (48) | 1·26 (0·20) |
| O(2) | −0·19013 (125) | 0·24785 (129) | 0·45347 (50) | 1·44 (0·21) |
| O(3) | 0·46868 (146) | 0·33401 (203) | 0·18721 (37) | 1·79 (0·29) |
| O(4) | 0 | 0 | 0 | 0·93 (0·30) |
| O(5) | 0·03358 (105) | −0·16436 (106) | 0·12344 (43) | 1·05 (0·18) |

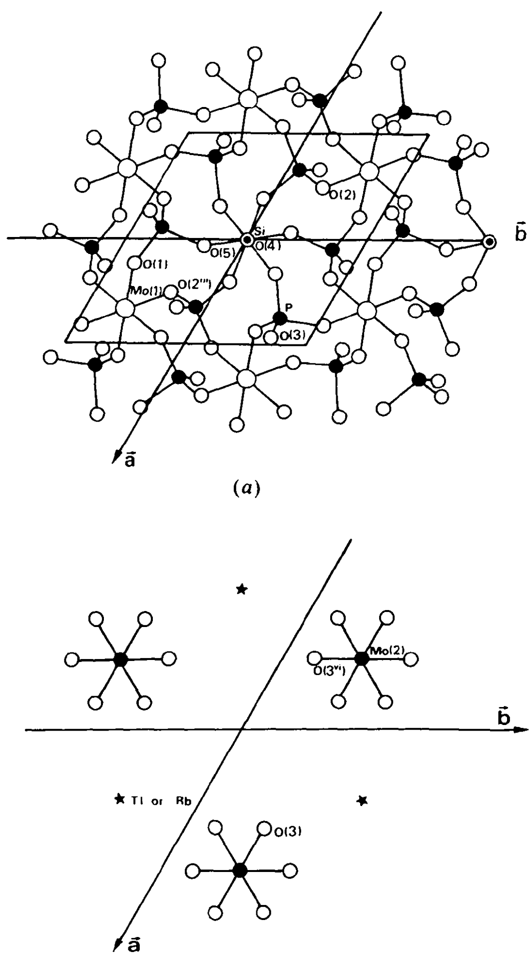


(*a*)

(*b*)

Fig. 1. Projections of the atoms (*a*) with $-0{\cdot}19 < z < 0{\cdot}19$ and (*b*) with $0{\cdot}18 < z < 0{\cdot}32$.

[010] where the $Tl^+$ and $Rb^+$ ions are located (Fig. 2). $SiO_4$ tetrahedra appear in the form of pyrosilicate groups with a staggered configuration; these $Si_2O_7$ groups share their six corners with $PO_4$ tetrahedra, forming 'tetrahedral' $[Si_2P_6O_{25}]$ units (Fig. 3). These units form columns along [001], two successive units being rotated by about 18° with respect to each other. These tetrahedral units are linked to each other through the corners of the $MoO_6$ octahedra, the ternary axis of which is parallel to [001]. The framework of this structure can also be described as $Mo_3P_6O_{30}$ strings formed of corner-sharing $PO_4$ and $MoO_6$ polyhedra directed along [001] (Fig. 4) which are linked together through $Si_2O_7$ groups and the free corners of the polyhedra.

The different polyhedra of the host lattice are almost regular as shown by Tables 2, 3, 4 and 5 which give the interatomic distances and angles. The two $MoO_6$ octahedra indeed exhibit very homogeneous distances (1·974 to 2·059 Å) very close to those observed for $MoO_2$ (Magnéli & Andersson, 1955) (1·94 to 2·07 Å), the O–Mo–O angles always being close to 90 or 180°. This in agreement with oxidation state IV for Mo in this phase which involves a symmetrical configuration of Mo, unlike $Mo^{VI}$ and $Mo^{V}$.

The $PO_4$ and $SiO_4$ tetrahedra are almost regular (Tables 4, 5) but the P and the Si atoms are respectively off center by about 0·084 and 0·037 Å for the Rb compound and by about 0·076 and 0·027 Å for the Tl compound. The P–O distances of the P–O–Si bonds are close to those (1·56 to 1·60 Å) observed for the P–O–P bonds in $Rb_{1\cdot6}P_8W_{32}O_{112}$, $Rb_{1\cdot8}P_8W_{24}O_{88}$ (Giroult *et al.*, 1980, 1981*a*) and $NaFeP_2O_7$ (Gabelica-Robert, Goreaud, Labbé & Raveau, 1982); however, they are longer than the P–O distances of the P–O–Mo bonds (1·502 to 1·526 Å).

Table 2. *Distances* (Å) *and OMO angles* (°) *for the* $Mo(1)O_6$ *octahedron*

Rb compound first line; Tl compound second line.

| | O(1) | O(1$^{i}$) | O(1$^{ii}$) | O(2$^{iii}$) | O(2$^{iv}$) | O(2$^{v}$) |
|---|---|---|---|---|---|---|
| Mo(1) | 2·044 (4)<br>2·043 (9) | 2·044 (4)<br>2·043 (9) | 2·044 (4)<br>2·043 (9) | 2·059 (4)<br>2·046 (12) | 2·059 (4)<br>2·046 (12) | 2·059 (4)<br>2·046 (12) |
| O(1) | | 2·778 (5)<br>2·78 (1) | 2·778 (5)<br>2·78 (1) | 2·931 (5)<br>2·92 (1) | 2·991 (5)<br>2·99 (1) | |
| O(1$^{i}$) | 85·6 (1)<br>85·7 (4) | | 2·778 (5)<br>2·78 (1) | | 2·931 (5)<br>2·92 (1) | 2·991 (5)<br>2·99 (1) |
| O(1$^{ii}$) | 85·6 (1)<br>85·7 (4) | 85·6 (1)<br>85·7 (4) | | 2·991 (5)<br>2·99 (1) | | 2·930 (5)<br>2·92 (1) |
| O(2$^{iii}$) | 91·2 (2)<br>91·2 (4) | 176·8 (1)<br>177·0 (4) | 93·6 (1)<br>93·9 (3) | | 2·900 (6)<br>2·87 (2) | 2·900 (6)<br>2·87 (2) |
| O(2$^{iv}$) | 93·6 (1)<br>93·9 (3) | 91·2 (2)<br>91·2 (4) | 176·8 (1)<br>177·0 (4) | 89·6 (1)<br>89·2 (4) | | 2·900 (6)<br>2·87 (2) |
| O(2$^{v}$) | 176·8 (1)<br>177·0 (4) | 93·6 (1)<br>93·9 (3) | 91·2 (2)<br>91·2 (4) | 89·6 (1)<br>89·2 (4) | 89·6 (1)<br>89·2 (4) | |

Symmetry code: (i) $-y, x-y-1, z$; (ii) $1+y-x, -x, z$; (iii) $y, x, z-0\cdot5$; (iv) $-x, y-x-1, z-0\cdot5$; (v) $x-y+1, -y, z-0\cdot5$; (vi) $-y, x-y, z$; (vii) $y-x, y, 0\cdot5-z$; (viii) $1-x, y, z$; (ix) $y-x, 1-x, z$; (x) $-y, 1-x, 0\cdot5-z$; (xi) $x-1, x-y, 0\cdot5-z$; (xii) $y-x, y, 0\cdot5-z$; (xiii) $y-x, -x, z$.

Table 3. *Distances* (Å) *and OMO angles* (°) *for the* $Mo(2)O_6$ *octahedron*

Rb first line; Tl second line.

| | O(3$^{viii}$) | O(3$^{vi}$) | O(3$^{ix}$) | O(3$^{x}$) | O(3$^{xi}$) | O(3$^{xii}$) |
|---|---|---|---|---|---|---|
| Mo(2) | 1·986 (5)<br>1·97 (1) | 1·986 (5)<br>1·97 (1) | 1·986 (5)<br>1·97 (1) | 1·986 (5)<br>1·97 (1) | 1·986 (5)<br>1·97 (1) | 1·986 (5)<br>1·97 (1) |
| O(3$^{viii}$) | | 2·864 (8)<br>2·85 (2) | 2·864 (8)<br>2·85 (2) | 2·752 (5)<br>2·73 (1) | 2·749 (7)<br>2·74 (2) | |
| O(3$^{vi}$) | 92·3 (2)<br>92·2 (5) | | 2·864 (8)<br>2·85 (2) | | 2·752 (5)<br>2·73 (1) | 2·749 (7)<br>2·74 (2) |
| O(3$^{ix}$) | 92·3 (2)<br>92·2 (5) | 92·3 (2)<br>92·2 (5) | | 2·749 (7)<br>2·74 (2) | | 2·752 (5)<br>2·73 (1) |
| O(3$^{x}$) | 87·7 (2)<br>87·6 (6) | 179·9 (2)<br>179·7 (7) | 87·6 (1)<br>88·0 (4) | | 2·864 (8)<br>2·85 (2) | 2·864 (8)<br>2·85 (2) |
| O(3$^{xi}$) | 87·6 (1)<br>88·0 (4) | 87·7 (2)<br>87·6 (6) | 179·9 (2)<br>179·7 (6) | 92·3 (2)<br>92·2 (5) | | 2·864 (8)<br>2·85 (2) |
| O(3$^{xii}$) | 179·9 (2)<br>179·7 (6) | 87·6 (1)<br>88·0 (4) | 87·7 (2)<br>87·6 (6) | 92·3 (2)<br>92·2 (5) | 92·3 (2)<br>92·2 (5) | |

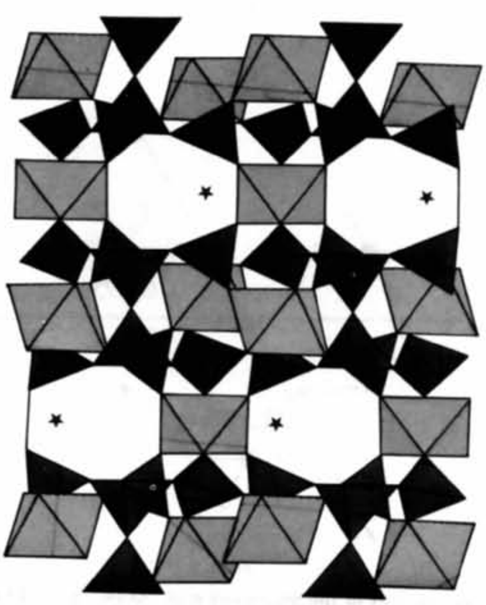

Fig. 2. Projection of the structure along **a** showing the tunnels.

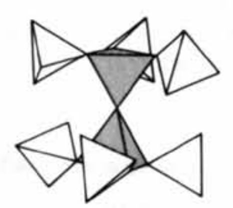

Fig. 3. The tetrahedral unit $Si_2P_6O_{25}$.

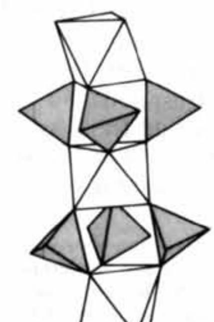

Fig. 4. The $Mo_3P_6O_{30}$ string.

Table 4. *Distances* (Å) *and* OSiO *angles* (°) *for the* $SiO_4$ *tetrahedron*

Rb first line; Tl second line.

| | O(4) | O(5) | $O(5^{vi})$ | $O(5^{xiii})$ |
|---|---|---|---|---|
| Si | 1·583 (2)<br>1·587 (4) | 1·614 (4)<br>1·621 (10) | 1·614 (4)<br>1·621 (10) | 1·614 (4)<br>1·621 (10) |
| O(4) | | 2·634 (4)<br>2·635 (9) | 2·634 (4)<br>2·635 (9) | 2·634 (4)<br>2·635 (9) |
| O(5) | 111·0 (1)<br>110·4 (3) | | 2·611 (5)<br>2·632 (14) | 2·611 (5)<br>2·632 (14) |
| $O(5^{vi})$ | 111·0 (1)<br>110·4 (3) | 108·0 (2)<br>108·5 (4) | | 2·611 (5)<br>2·632 (14) |
| $O(5^{xiii})$ | 111·0 (1)<br>110·4 (3) | 108·0 (2)<br>108·5 (4) | 108·0 (2)<br>108·5 (4) | |

Table 5. *Distances* (Å) *and* OPO *angles* (°) *for the* $PO_4$ *tetrahedron*

Rb first line; Tl second line.

| | $O(1^{vi})$ | $O(2^{vii})$ | O(3) | $O(5^{vi})$ |
|---|---|---|---|---|
| P | 1·509 (5)<br>1·502 (12) | 1·509 (3)<br>1·511 (9) | 1·513 (4)<br>1·526 (9) | 1·579 (3)<br>1·564 (9) |
| $O(1^{vi})$ | | 2·545 (5)<br>2·54 (1) | 2·453 (7)<br>2·46 (1) | 2·485 (6)<br>2·46 (2) |
| $O(2^{vii})$ | 115·0 (2)<br>115·0 (5) | | 2·531 (5)<br>2·53 (1) | 2·484 (5)<br>2·48 (1) |
| O(3) | 108·6 (3)<br>108·5 (7) | 113·7 (3)<br>112·9 (8) | | 2·447 (5)<br>2·45 (1) |
| $O(5^{vi})$ | 107·2 (2)<br>106·9 (5) | 107·0 (2)<br>107·7 (6) | 104·7 (2)<br>105·1 (5) | |

In a similar way the Si–O distances corresponding to the P–O–Si bonds are close to those given by Baur (1977) for different silicates, and are longer than the Si–O distances of the Si–O–Si bonds. The tunnels can be considered as resulting from the stacking of several sorts of rings: almost planar rings formed of four octahedra and eight tetrahedra $[(MoO_6)_4(SiO_4)_2(PO_4)_6]$ (Fig. 5*a*) and which are strongly inclined with respect to the axis of the tunnels; rings built up from three octahedra and five tetrahedra $[(MoO_6)_3(SiO_4)(PO_4)_4]$ (Fig. 5*b*); and rings built up from two octahedra and six tetrahedra (Fig. 5*c*) whose mean plane is closer to the plane normal to the axis of the tunnels.

The geometry of these latter two windows exhibits some analogy with that of $Cs_2Nb_4O_{11}$ (Gasperin, 1981) (Fig. 6), although formed of different polyhedra, and can thus be described as being derived from the hexagonal rings observed in the pyrochlore structure by the addition of two polyhedra (Fig. 6). This analogy with the pyrochlore structure and with octahedral structures resulting from the intergrowth of pyrochlore with the $A_2Nb_6TiO_{18}$ structures (Michel, Guyomarc'h & Raveau, 1977, 1978; Michel, Guyomarc'h, Deschanvres & Raveau, 1978; Marini, Michel & Raveau, 1979; Desgardin, Robert, Groult & Raveau, 1977) is also observed as regards the orientation of the tunnels which extend along three directions, [100], [010] and [110], so that three tunnels belonging to the same (001) plane intersect at the level of the same cage; this characteristic is very similar to that observed for the titanoniobate $A_2TiNb_6O_{18}$ (Desgardin *et al.*, 1977); only the tunnels of the same level can communicate with each other allowing an eventual mobility of the *A* ions in the (001) plane, unlike the pyrochlores for which a three-dimensional migration of the *A* ions is possible, owing to the presence of additional tunnels in other directions. Thus, these tunnels form very voluminous cages and, as a result, $Tl^+$ and $Rb^+$ which are located at the center of an antiprism formed by the faces of two $MoO_6$ octahedra lying along **c** exhibit minimum Tl–O and Rb–O distances [3·147 (9) and 3·142 (4) Å respectively] which are greater than usually observed. This characteristic is in agreement with the high anisotropic thermal parameter observed along the ⟨100⟩ and ⟨110⟩ directions, *i.e.* along the axes of the tunnels. Thus it appears that this type of structure should allow the possibility of migration of the alkaline ions through the framework, and for this reason the ion-exchange properties of these compounds have been investigated as shown below.

Attention must be drawn to the problem of non-stoichiometry observed for these compounds: the presence of a small deficiency of P in the $PO_4$ tetrahedra is unusual but is necessary to ensure the charge balance, unless the composition is considered

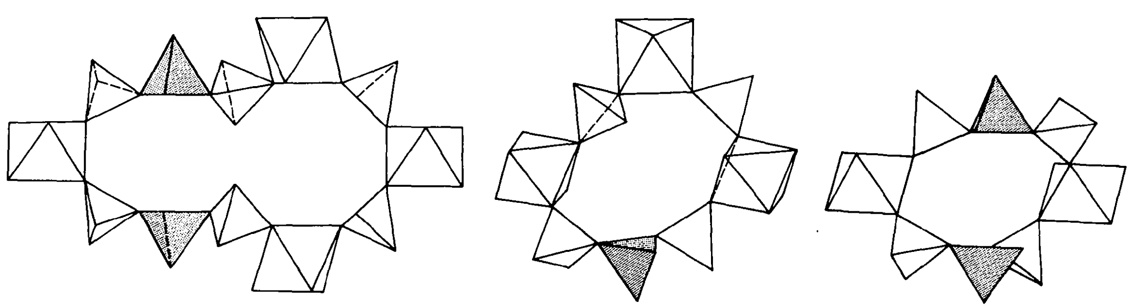

(*a*) (*b*) (*c*)

Fig. 5. (*a*) $[(MoO_6)_4(SiO_4)_2(PO_4)_6]$ ring. (*b*) $[(MoO_6)_3(SiO_4)(PO_4)_4]$ ring. (*c*) $[(MoO_6)_2(SiO_4)_2(PO_4)_4]$ ring.

to be $RbMo_2^{IV}Mo^{III}P_6Si_2O_{25}$; however, this latter hypothesis is less likely because the existence of $Mo^{III}$ has never been proved in oxides. Attempts to prepare stoichiometric oxides such as $RbMo_3^{IV}P_5Si_3O_{25}$ were unsuccessful; this is easily explained by the fact that Si and P cannot be distributed on the same tetrahedral sites owing to their different sizes. In the same way, the possibility of the existence of an Rb or a Tl deficiency has been considered: it has been observed that this structure can be formed without Rb or Tl, *i.e.* for the composition $Mo_3^{IV}P_6Si_2O_{25}$, but this phase always appears in a mixture of several oxides and could not be isolated. On the other hand, a compensation charge on the Mo sites, by partially substituting a trivalent cation for Mo, stabilizes this structure; so, for example, the compound $RbMo_2^{IV}Ti^{III}P_6Si_2O_{25}$ could be more easily prepared as a pure compound than the phase $RbMo_3^{IV}P_{5\cdot8}Si_2O_{25}$; however, single crystals of this phase have not been isolated up to the present.

### Ion-exchange properties

The ion-exchange properties of these oxides were studied in a first step in an aqueous medium. Two possibilities were investigated: proton exchange in an acidic medium, and exchange by $Na^+$ ions with a sodium chloride solution. About 1 g of these compounds was placed in a vacuum filter and the exchange solution was then added at different concentrations: 0·1, 1 and 5$M$; in the case of the acid solution three sorts of acids were successively used: $H_2SO_4$, HCl and $HNO_3$. Tl or Rb, and Na were then analyzed in both, the solid compounds after reaction and in the liquid phase. Whatever the starting oxide may be, and whatever the exchange solution, no ion-exchange properties were found under these experimental conditions, contrary to the results observed for several octahedral intersecting-tunnel structures such as pyrochlores (Michel, Hervieu & Raveau, 1971; Groult, Michel & Raveau, 1972; Michel, Groult, Deschanvres & Raveau, 1975*a*, *b*) and $A_2Nb_6TiO_{18}$-related oxides (Marini *et al.*, 1979; Robert, Desgardin & Raveau, 1979). In the same way, attempts at exchanging by placing the starting oxides in a vacuum filter and heating to 343 K in the presence of an appropriate solution were unsuccessful.

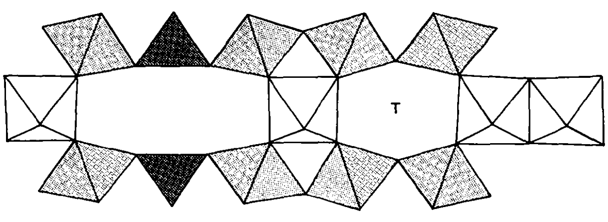


Fig. 6. Tunnels in the $Cs_2Nb_4O_{11}$ structure. $T$ indicates the hexagonal ring of a pyrochlore structure.

The ion-exchange properties were then studied in a second step according to a method which was first described by Michel, Robert, Groult & Raveau (1975) for the thallium pyrochlores and which is based on the volatility of thallium chloride at moderate temperature. Thus the $TlMo_3P_{5\cdot8}Si_2O_{25}$ oxide was mixed with sodium chloride and heated under primary vacuum at 673 K for different lengths of time. The ion-exchange products were analyzed by atomic absorption spectroscopy.

With these experimental conditions, different ion-exchange products were observed:

$$TlMo_3P_{5\cdot8}Si_2O_{25} + xNaCl \rightarrow Tl_{1-x}Na_xMo_3P_{5\cdot8}Si_2O_{25} + xTlCl$$

with $0 < x \leq 1$.

The Na compounds are hygroscopic and can absorb up to one $H_2O$ molecule per $Na^+$ ion without changing their structure. Thus it appears that these oxides exhibit ion-exchange properties in agreement with the presence of intersecting tunnels. The X-ray diffraction patterns of the sodium oxides do not exhibit a significant variation of the cell parameters, but the intensity of some reflections is drastically changed owing to the replacement of Tl by Na.

### References


BANKS, E. & GOLDSTEIN, A. (1968). *Inorg. Chem.* **7**, 966–969.
BAUR, W. H. (1977). *Acta Cryst.* B**33**, 2615–2619.
BENMOUSSA, A., LABBÉ, PH., GROULT, D. & RAVEAU, B. (1982). *J. Solid State Chem.* **44**, 318–325.
COPPENS, P. & HAMILTON, W. C. (1970). *Acta Cryst.* A**26**, 71–83.
COPPENS, P., LEISEROWITZ, L. & RABINOVICH, D. (1965). *Acta Cryst.* **18**, 1035–1038.
DESGARDIN, G., ROBERT, C., GROULT, D. & RAVEAU, B. (1977). *J. Solid State Chem.* **22**, 101–111.
DOMENGES, B., GOREAUD, M., LABBÉ, PH. & RAVEAU, B. (1982). *Acta Cryst.* B**38**, 1724–1728.
FUKUSHIMA, H. F., KOBAYASHI, A. & SASAKI, Y. (1981). *Acta Cryst.* B**37**, 1613–1615.
GABELICA-ROBERT, M., GOREAUD, M., LABBÉ, PH. & RAVEAU, B. (1982). *J. Solid State Chem.* **45**, 389–395.
GASPERIN, M. (1981). *Acta Cryst.* B**37**, 641–643.
GIROULT, J. P., GOREAUD, M., LABBÉ, PH. & RAVEAU, B. (1980). *Acta Cryst.* B**36**, 2570–2575.
GIROULT, J. P., GOREAUD, M., LABBÉ, PH. & RAVEAU, B. (1981*a*). *Acta Cryst.* B**37**, 1163–1166.
GIROULT, J. P., GOREAUD, M., LABBÉ, PH. & RAVEAU, B. (1981*b*). *Acta Cryst.* B**37**, 2139–2142.
GIROULT, J. P., GOREAUD, M., LABBÉ, PH. & RAVEAU, B. (1982*a*). *Acta Cryst.* B**38**, 2342–2347.
GIROULT, J. P., GOREAUD, M., LABBÉ, PH. & RAVEAU, B. (1982*b*). *J. Solid State Chem.* **44**, 407–414.
GROULT, D., MICHEL, C. & RAVEAU, B. (1972). *C.R. Acad. Sci. Sér. C*, **274**, 374–377.
HERVIEU, M. & RAVEAU, B. (1982). *J. Solid State Chem.* **43**, 299.
HERVIEU, M. & RAVEAU, B. (1983*a*). *Chem. Scr.* To be published.
HERVIEU, M. & RAVEAU, B. (1983*b*). *Chem. Scr.* To be published.
HUSSAIN, A. & KIHLBORG, L. (1976). *Acta Cryst.* A**32**, 551–557.
ICHIDA, H., KOBAYASHI, A. & SASAKI, Y. (1980). *Acta Cryst.* B**36**, 1382–1387.
*International Tables for X-ray Crystallography* (1974). Vol. IV. Birmingham: Kynoch Press.

KIERKEGAARD, P. (1962*a*). *Ark. Kemi*, **18**, 521–532.
KIERKEGAARD, P. (1962*b*). *Ark. Kemi*, **18**, 553–575.
KIERKEGAARD, P. (1962*c*). *Ark. Kemi*, **19**, 1–14.
KIERKEGAARD, P. & LONGO, J. M. (1970). *Acta Chem. Scand.* **24**, 427–432.
KIHLBORG, L. & KLUG, A. (1973). *Chem. Scr.* **3**, 207–211.
KIHLBORG, L. & SHARMA, R. (1982). *J. Microsc. Electron.* **7**, 387–396.
KIHLBORG, L., SUNDBERG, M. & HUSSAIN, A. (1980). *Chem. Scr.* **15**, 182–186.
LECLAIRE, A., MONIER, J. C. & RAVEAU, B. (1983). *J. Solid State Chem.* **48**, 147–153.
MAGNÉLI, A. (1949). *Ark. Kemi*, **1**, 213–221.
MAGNÉLI, A. (1953). *Acta Chem. Scand.* **7**, 315–324.
MAGNÉLI, A. & ANDERSSON, G. (1955). *Acta Chem. Scand.* **9**, 1378–1381.
MAGNÉLI, A. & BLOMBERG, B. (1951). *Acta Chem. Scand.* **5**, 372–378.
MARINI, A., MICHEL, C. & RAVEAU, B. (1979). *Rev. Chim. Minér.* **16**, 73–79.
MEULENAER, J. DE & TOMPA, H. (1965). *Acta Cryst.* **19**, 1014–1018.
MICHEL, C., GROULT, D., CHAILLEUX, J. M. & RAVEAU, B. (1976). *Rev. Chim. Minér.* **13**, 283–289.
MICHEL, C., GROULT, D., DESCHANVRES, A. & RAVEAU, B. (1975*a*). *J. Inorg. Nucl. Chem.* **37**, 251–255.
MICHEL, C., GROULT, D., DESCHANVRES, A. & RAVEAU, B. (1975*b*). *J. Inorg. Nucl. Chem.* **37**, 1957–1959.
MICHEL, C., GUYOMARC'H, A., DESCHANVRES, A. & RAVEAU, B. (1978). *Mater. Res. Bull.* **13**, 197–203.
MICHEL, C., GUYOMARC'H, A. & RAVEAU, B. (1977). *J. Solid State Chem.* **22**, 393–403.
MICHEL, C., GUYOMARC'H, A. & RAVEAU, B. (1978). *J. Solid State Chem.* **25**, 251–261.
MICHEL, C., HERVIEU, M. & RAVEAU, B. (1971). *Bull. Soc. Chim. Fr.* pp. 3939–3943.
MICHEL, C., ROBERT, C., GROULT, D. & RAVEAU, B. (1975). *Mater. Res. Bull.* **10**, 949–955.
MINACHEVA, L. KH., ANTSYSHKINA, A. S., LAVROV, A. V., SAKHAROVA, U. G., NIKOLAEV, V. P. & PORAI-KOSHITS, M. A. (1979). *Zh. Neorg. Khim.* **24**, 91–93.
ROBERT, C., DESGARDIN, G. & RAVEAU, B. (1979). *J. Inorg. Nucl. Chem.* **41**, 893–894.
SWANSON, A. B. & ANDERSON, J. S. (1968). *Mater. Res. Bull.* **3**, 149–157.
WANLASS, D. R. & SIENKO, M. J. (1975). *J. Solid State Chem.* **12**, 362–369.

*Acta Cryst.* (1984). B**40**, 185–191

# Tetragonal Tetrahedra Distortions in Cubic Sodalite Frameworks

BY W. DEPMEIER

*Chimie Appliquée, Université, Sciences* II, 30 *quai E. Ansermet, CH* 1211 *Genève, Switzerland*

(*Received* 29 *June* 1983; *accepted* 11 *November* 1983)

## Abstract

A literature search for sodalite frameworks has revealed that, besides tilting, tetrahedron-edge-length distortions are an important means of releasing strains imposed by geometrical constraints. The extent of this distortion rises with the Al content in the series of framework composition $[Al_{12-n}Si_nO_{24}]^{(12-n)-}$ ($0\leq n\leq 12$). Violations of Loewenstein's rule are connected with large tetrahedron-edge-length distortions. Geometrical relationships are given.

## Introduction

The general formula for members of the sodalite family is $M_8[T_{12}O_{24}]X_2$. Tetrahedra $TO_4$ with $T = Si^{4+}, Al^{3+}, Be^{2+}, B^{3+},\ldots$ are connected with each other *via* common O atoms to form what is known as the sodalite framework. The centres of the tetrahedra occupy thereby the corners of truncated octahedra which in turn, being linked by common 4-rings and 6-rings, form a space-filling arrangement. The $T$ cations need not be all of the same kind in a given structure. In fact, a sodalite framework with only Si has never been found (it would be a hypothetical silica modification). Usually, part of the tetravalent $Si^{4+}$ is replaced by other lower-charged cations (most commonly $Al^{3+}$) and the framework composition becomes, *e.g.*, $[Al_6Si_6O_{24}]^{6-}$. Clearly, this framework needs charge compensation to maintain electroneutrality. This is achieved by balancing the negative charges of the framework by a combination of cations and anions being situated in the large cavities (cages) formed by the framework. Besides charge balancing, these cage cations $M$ (typically $Na^+$, $K^+$, $Ca^{2+},\ldots$) and cage anions $X(Cl^-, SO_4^{2-},\ldots)$ have another important function as they prevent the open tetrahedra framework from collapsing. They serve as a form of spacer and when they are smaller than the size corresponding to a maximal expansion, the framework adapts itself to the size of the cage ions. Pauling (1930), who determined the structure of the natural mineral sodalite, called this volume reduction a 'partial collapse'. The mechanism by which the framework reduces its cage volume consists of cooperative rotations of the $TO_4$ tetrahedra about their $\bar{4}$ axes. Fig. 1 of Taylor (1972) illustrates very clearly this tilting or folding of the sodalite framework. The degree of tilting is measured by the tilt angle $\varphi$.

0108-7681/84/030185-07\$01.50 